A Mach-Zehnder interferometer electro-optic switch with ultralow voltage-length product using poled-polymer/ silicon slot waveguide*

HUANG Xiao-liang (黄小亮), **LI Cui-ting** (李翠婷), **DANG Pei-pei** (党佩佩), **and ZHENG Chuan-tao** (郑传涛)**

State Key Laboratory on Integrated Optoelectronics, College of Electronic Science and Engineering, Jilin University, Changchun 130012, China

(Received 7 May 2015)

By using poled-polymer/silicon slot waveguides in the active region and the Pockels effect of the poled-polymer, we propose a kind of Mach-Zehnder interferometer (MZI) electro-optic (EO) switch operated at 1 550 nm. Structural parameters are optimized for realizing normal switching function. Dependencies of switching characteristics on the slot waveguide parameters are investigated. For the silicon strip with dimension of 170 nm×300 nm, as the slot width varies from 50 nm to 100 nm, the switching voltage can be as low as 1.0 V with active region length of only 0.17–0.35 mm, and the length of the whole device is only about 770–950 μm. The voltage-length product of this switching structure is only 0.17–0.35 V·mm, and it is at least 19–40 times smaller than that of the traditional polymer MZI EO switch, which is 6.69 V·mm. Compared with our previously reported MZI EO switches, this switch exhibits some superior characteristics, including low switching voltage, compact device size and small wavelength dependency.

Document code: A **Article ID:** 1673-1905(2015)04-0264-4

DOI 10.1007/s11801-015-5081-3

In recent years, optical switching devices have received more and more attention due to their wide applications in optical communication and optical signal processing systems. In our previous reports, based on rib/rectangular waveguides and the poled polymer AJ309[1,2], different non-resonant electro-optic (EO) switches have been numerically proposed, and they usually exhibit a switching voltage of 2–5 V and an EO region length of 3–6 mm, which indicates a voltage-length product of 5–30 V·mm[3-5]. For a lower EO coefficient, a long active region is required to drop the switching voltage below 1 V, but this will lead to long waveguide length, which is not allowed in low-voltage, ultra-compact and chip-level interconnection. Besides polymer EO switches, silicon EO switches also have shown great potential for being compatible with standard complementary metal-oxide-semiconductor (CMOS) processing technology. So far, silicon EO switches have been widely demonstrated based on free carrier depletion[6-8] or injection[9,10] in diode structures or CMOS structures[11]. To meet the needs of optical communication, an optical switch should possess some important characteristics, involving small device dimension, suitable electrical and optical bandwidth, large voltage-length product, high extinction ratio and low power consumption.

Compared with other waveguide structures, such as rib waveguide and rectangular waveguide, the slot waveguide has been proven to be a good candidate to design and fabricate integrated optical devices. In this paper, we propose a kind of Mach-Zehnder interferometer (MZI) EO switch operated at 1 550 nm by using poled-polymer/ silicon slot waveguides in the active region and silicon waveguides in the passive region, and the Pockels effect is exploited via the poled-polymer cladding in the slot waveguide. Through optimization, the device can perform normal switching functions. An impressive advantage of this structure is that its voltage-length product is reduced by at least 19–40 times compared with that of the polymer MZI EO switch with switching voltage of 2.23 V and EO region length of 3 mm[12].

Fig.1(a) shows the detailed structure of the EO switch, which consists of an input 3 dB directional coupling region with a length of L_1, an output 3 dB directional coupling region with a length of L_1, an MZI EO region composed by two slot waveguides with a length of L_{MZI}, and two transitive regions containing four sinusoidal transitive waveguides with a length along the propagation of L_2. The cross-section of the left MZI EO arm is

* This work has been supported by the National Natural Science Foundation of China (Nos.61107021, 61177027 and 61077074), the Ministry of Education of China (Nos.20110061120052 and 20120061130008), and the Science and Technology Department of Jilin Province of China (No.20130522161JH).

** E-mail: zhengchuantao@jlu.edu.cn

shown in Fig.1(b). The slot waveguide contains an under silica cladding layer, two silicon strips with thin strip loader, a poled-polymer slot and an upper poled-polymer cladding layer. At wavelength of 1 550 nm, the EO coefficient of the poled polymer is γ_{33}=138 pm/V, the amplitude loss coefficient is 2.0 dB/cm, and the refractive index is n_1=1.58. Then the mode effective refractive index can be tuned through changing the applied voltage. The refractive indices of silicon and silica are n_2=3.455 and n_3=1.46, respectively. The widths of silicon strip width and slot are W_d and W_s, respectively. The thicknesses of under silica cladding, slot and upper polymer cladding are h_1, h and h_2, respectively. The thickness of silicon strip loader on top of the silica layer is h_3.

In the two directional coupling regions, each 3 dB coupler contains two directional coupling silicon rectangular waveguides. The cross-section view in the coupling region is shown in Fig.1(c). The waveguide width and height are defined as W and H, respectively, and $H=h+h_3$, h_3 =50 nm. The coupling gap between the two silicon waveguides is d. In order to realize the mode conversion between rectangular waveguide and slot waveguide, four taper-like coupling waveguides are used, as shown in the inset of Fig.1(a).

In the MZI EO region, the deposited electrodes contain three parts, left electrode, center electrode and right electrode. For obtaining a push-pull operation in the two arms, the EO polymers in the two slot areas are poled using contact poling method along the same direction. During poling, the three poling voltages applied on the left electrode, the center electrode and the right electrode are $+U_{pol}$, 0 V and $-U_{pol}$, respectively, and these three voltages during operation are 0 V, U and 0 V, respectively.

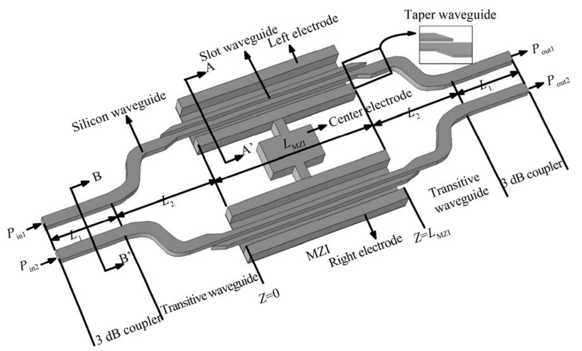

(a)

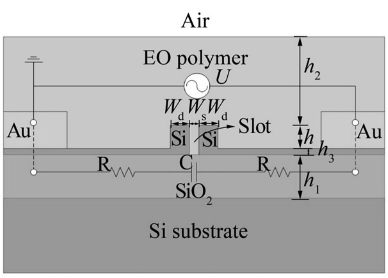

(b)

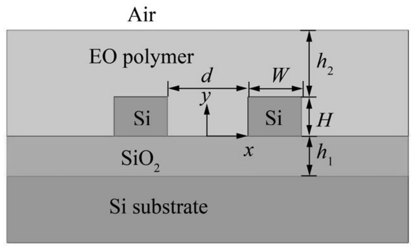

(c)

Fig.1 (a) Structure of the MZI EO switch based on slot waveguide; (b) Cross-section view from AA' side of the slot waveguide in the MZI region; (c) Cross-section view from BB' side in the 3 dB directional coupling region

In the following design, the operation wavelength of the device is selected as 1 550 nm. Since the external applied electric field is along the x direction, the optical mode is selected as TE mode. The slot waveguide and the silicon rectangular waveguide should be both single-mode waveguides, so we need to optimize the waveguide core parameters. For slot waveguide, under TE polarization, the curves of effective refractive indices of the TE_0 and TE_1 modes versus the silicon width W_d are shown in Fig.2(a), where λ=1 550 nm, W_s=100 nm, $h_1=h_2$=1 000 nm, h_3=50 nm and h=300 nm. It can be seen that when W_d is taken as smaller than 250 nm, the single mode propagation can be realized under TE polarization. For silicon rectangular waveguide, under TE polarization, the curves of the effective refractive indices of TE_0 and TE_1 modes versus the silicon width W are shown in Fig.2(b), where λ=1 550 nm, $h_1=h_2$=1 000 nm and H=350 nm. It can be seen that when W is taken as smaller than 410 nm, the single mode propagation can be assured under TE polarization.

With wavelength of 1 550 nm, for the two directional coupling silicon waveguides, Fig.3(a) shows the curves of the effective refractive indices of symmetric TE_0 mode (denoted as $N_{ref,s}$) and asymmetric TE_1 mode (denoted as $N_{ref,a}$) versus the coupling gap d. We can observe from Fig.3(a) that $N_{ref,s}$ decreases and $N_{ref,a}$ increases with the increase of d, and they gradually approach an identical value. Using

$$L_1=\frac{L_c}{2}=\frac{\lambda}{2\left[N_{ref,s}(d,\lambda)-N_{ref,a}(d,\lambda)\right]}, \tag{1}$$

the relation between the coupling region length L_1 and the gap d is shown Fig.3(b). When d is less than 0.6 μm, L_1 is less than 500 μm. In order to enhance the coupling of 3 dB coupler, reduce the length L_1 and improve the device integrality, d should be taken as small as possible. However, d cannot be taken too small. Otherwise, these two coupling waveguides will be converted into a slot waveguide. Therefore, we select the coupling gap as d=400 nm, and the corresponding coupling region length is about L_1=97.5 μm.

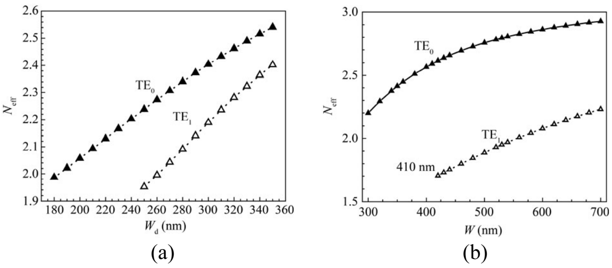

Fig.2 Curves of the effective refractive indices of TE$_0$ and TE$_1$ modes versus (a) the silicon strip width W_d in the slot waveguide and (b) the silicon waveguide width W in the silicon rectangular waveguide

EO overlap integral Γ_x clearly shows the modulation efficiency of an EO switch, and it should be as large as possible in order to reduce the switching voltage. Under 1 550 nm wavelength, Fig.4 shows the curves of Γ_x versus the parameters of slot waveguide. With the increase of slot width W_s, the electric field in the slot drops, and Γ_x exhibits an obvious decreasing trend. With the increase of h or W_d, the electric field in the slot is almost constant, and therefore Γ_x exhibits an increasing trend. Thus, enlarging the silicon width and minimizing the slot width can be both effective to increase Γ_x, which will be helpful for minimizing the switching voltage as well as shortening the EO region length.

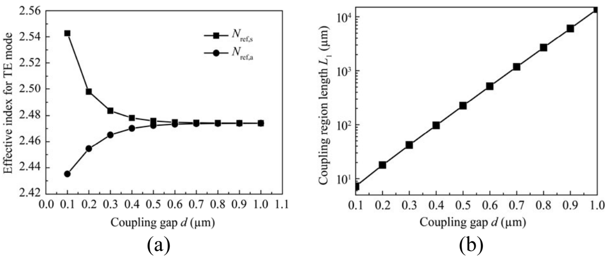

Fig.3 For the two directional coupling silicon waveguides, curves of (a) the effective refractive indices of TE$_0$ and TE$_1$ modes and (b) the coupling region length L_1 of the 3 dB silicon directional coupler versus the coupling gap *d*

The product of the switching voltage U_s and L_{MZI} is an important characteristic for the MZI switch. Fig.5 shows the curves of $U_s \times L_{MZI}$ with different slot waveguide parameters. We can see from Fig.5 that the product gets larger with the increase of W_s, and a small W_s is required to drop the switching voltage and shorten the EO region length. The larger the silicon height h, the lower the product of $U_s \times L_{MZI}$, and this phenomenon can be explained according to the relation between Γ_x and h as shown in Fig.4(a). From Fig.5(b), to a certain extent, the product of $U_s \times L_{MZI}$ is lower with a wider W_d, and it will finally become a saturation value when W_d reaches the width of 210 nm. This phenomenon can be explained according to the relation between Γ_x and W_d as shown in Fig.4(b). Besides, the dependency of the product on wavelength is further investigated as depicted in Fig.5(c). The product varies slightly with wavelength. This is due to the slight variation of the power ratio confined in the slot with the change of operation wavelength.

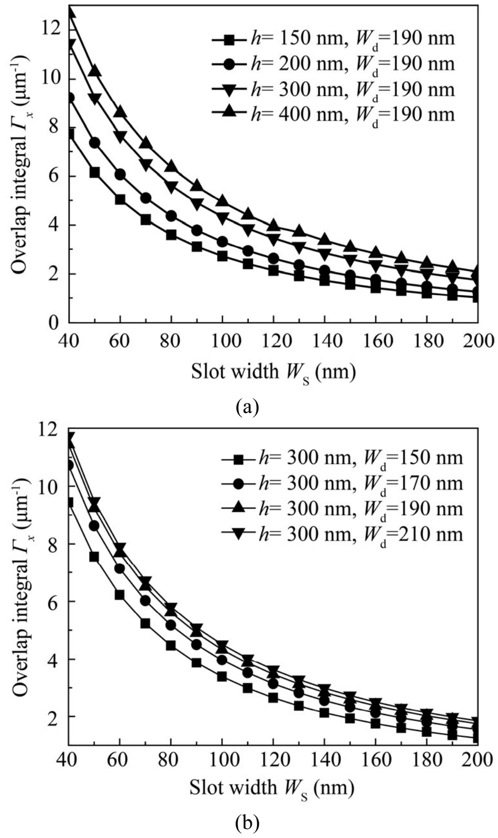

Fig.4 Curves of the EO overlap integral Γ_x versus the slot width W_s with (a) the same W_d and different *h* and (b) the same *h* and different W_d

Based on the above discussion, in order to decrease the voltage-length product, we should choose a smaller W_s, a larger h and a larger W_d. For example, we can take $W_d \times h$ as 190 nm×300 nm, and in this case, when the slot width is W_s=50 nm, the corresponding $U_s \times L_{MZI}$ is 170.5 V·μm. In a similar way, when W_s=100 nm, the corresponding $U_s \times L_{MZI}$=351.0 V·μm. Taking the switching voltage as 1.0 V, the total length of the switch is 770 μm (including two 97.5 μm-long couplers, a 200 μm-long transitive region and a 170 μm-long MZI region) with slot width of 50 nm, and that is 950 μm (including two 97.5 μm-long couplers, a 200 μm-long transitive region and a 350 μm-long MZI region) with slot width of 100 nm.

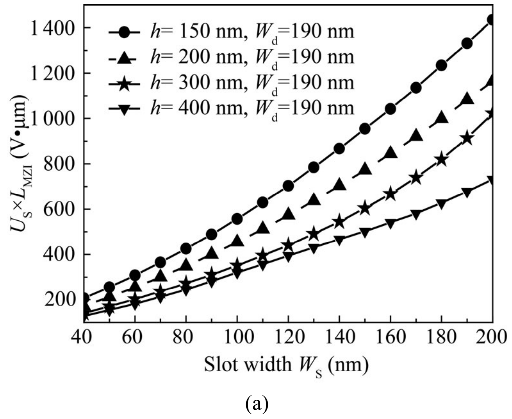

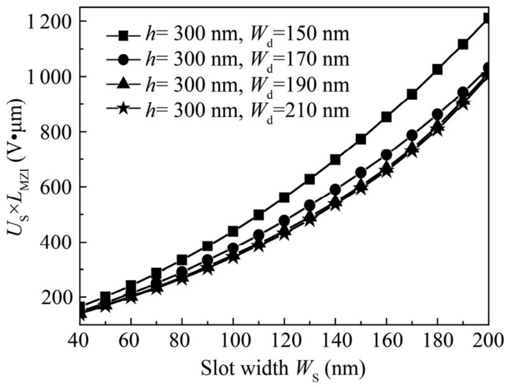

(b)

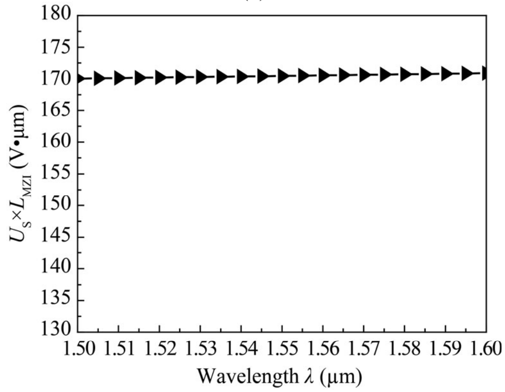

(c)

Fig.5 Curves of the voltage-length product $U_s \times L_{MZI}$ versus the slot width W_s with (a) the same W_d and different h and (b) the same h and different W_d; (c) Curve of the voltage-length product $U_s \times L_{MZI}$ versus operation wavelength λ with $W_s \times W_d \times h$ =50 nm×190 nm×300 nm

Through using poled-polymer/silicon slot waveguides and employing the Pockels effect of the poled-polymer, a kind of MZI EO switch operated at 1 550 nm is proposed. Structural design and simulation are performed. With the silicon strip dimension of 190 nm×300 nm, as the slot width varies from 50 nm to 100 nm, the switching voltage can be as low as 1.0 V with active region length of only 0.17–0.35 mm. The whole device length is less than 650 μm when the slot width is 100 nm, or less than 470 μm with the slot width of 50 nm. The voltage-length product of the proposed device is only 0.17–0.35 V·mm, which is reduced by at least 19–40 times compared with that of our previously reported traditional polymer MZI EO switch (6.69 V·mm). Due to the compact size and the ultra-low switching voltage, the switch can be good candidate for implementing the functions of optical switching and optical routing in optical network-on-chip fields.

References

[1] Y. Enami, C. T. Derose, D. Mathine, C. Loychik, C. Greenlee, R. A. Norwood, T. D. Kim, J. Luo, Y. Tian, A. K. Y. Jen and N. Peyghambarian, Nature Photonics **1**, 180 (2007).

[2] Y. Enami, D. Mathine, C. T. DeRose, R. A. Norwood, J. Luo, A. Y. Jen and N. Peyghambarian, Applied Physics Letters **91**, 093505 (2007).

[3] C. T. Zheng, C. S. Ma, X. Yan, X. Y. Wang and D. M. Zhang, Optics Communications **281**, 5998 (2008).

[4] C. T. Zheng, C. S. Ma, X. Yan, X. Y. Wang and D. M. Zhang, Applied Physics B **96**, 95 (2009).

[5] C. T. Zheng, C. S. Ma, X. Yan, X. Y. Wang and D. M. Zhang, Journal of Modern Optics **56**, 1383 (2009).

[6] Q. Xu, B. Schmidt, S. Pradhan and M. Lipson, Nature **435**, 325 (2005).

[7] D. J. Thomson, F. Y. Gardes, J. M. Fedeli, S. Zlatanovic, Y. Hu, B. P. P. Kuo, E. Myslivets, N. Alic, S. Radic, G. Z. Mashanovich and G. T. Reed, IEEE Photonics Technology Letters **24**, 234 (2012).

[8] P. Dong, S. Liao, D. Feng, H. Liang, D. Zheng, R. Shafiiha, C. C. Kung, W. Qian, G. L. Li, X. Z. Zheng, A. V. Krishnamoorthy and M. Asghari, Optics Express **17**, 22484 (2009).

[9] W. M. Green, M. J. Rooks, L. Sekaric and Y. A. Vlasov, Optics Express **15**, 17106 (2007).

[10] R. Palmer, L. Alloatti, D. Korn, P. C. Schindler, M. Baier, J. Bolten, T. Wahlbrink, M. Waldow, R. Dinu, W. Freude, C. Koos and J. Leuthold, IEEE Photonics Technology Letters **25**, 1226 (2013).

[11] J. Fujikata, J. Ushida, Y. Ming-Bin, Z. ShiYang, D. Liang, P. L. Guo-Qiang, K. Dim-Lee and T. Nakamura, 25 GHz Operation of Silicon Optical Modulator with Projection MOS Structure, Conference on Optical Fiber Communication (OFC), collocated National Fiber Optic Engineers Conference, 1 (2010).

[12] C. T. Zheng, C. S. Ma, X. Yan, X. Y. Wang and D. M. Zhang, Optics & Laser Technology **42**, 457 (2010).